Acta Biochim Biophys Sin 2011, 43: 867–876 | © The Author 2011. Published by ABBS Editorial Office in association with Oxford University Press on behalf of the Institute of Biochemistry and Cell Biology, Shanghai Institutes for Biological Sciences, Chinese Academy of Sciences. DOI: 10.1093/abbs/gmr081.
Advance Access Publication 10 September 2011

Original Article

Biophysical characterization of calmodulin and calmodulin-like proteins from rice, *Oryza sativa* L.

Aumnart Chinpongpanich, Nuchanat Wutipraditkul, Sarut Thairat, and Teerapong Buaboocha*

Department of Biochemistry, Faculty of Science, Chulalongkorn University, Bangkok 10330, Thailand
*Correspondence address. Tel: +66-22185436; Fax: +66-22185418; E-mail: Teerapong.B@Chula.ac.th

Calmodulin (CaM) transduces the increase in cytosolic Ca^{2+} concentrations by binding to and altering the activities of target proteins, thereby affecting the physiological responses to the vast array of stimuli. Here, we examined the purified recombinant proteins encoded by three *Cam* and eight *Cam-like* (*CML*) genes from rice. With the exception of one OsCML, all recombinant proteins could be purified by Ca^{2+}-dependent hydrophobic chromatography and exhibited an electrophoretic mobility shift when incubated with Ca^{2+}. The three CaMs all bound CaM kinase II peptide, but none of the eight CMLs did, suggesting a possible differential target binding between the CaM and CML proteins. In addition, their conformational changes upon Ca^{2+}-binding were evaluated by circular dichroism spectroscopy and fluorescence spectroscopy using 8-Anilino-1-naphthalene-sulfonic acid. Taken together, OsCMLs were found exhibiting a spectrum of both structural and functional characteristics that ranged from typical to atypical of CaMs. From structural comparison, the OsCMLs have overall main-chain conformation nearly identical to OsCaMs, but with distinct distribution of some charged and hydrophobic amino acids on their target-binding site. These results suggest that genetic polymorphism has promoted the functional diversity of the OsCML family, whose members possess modes of actions probably different from, though maybe overlapping with, those of OsCaMs.

Keywords calcium signaling; calmodulin; CaM; CML; rice

Received: May 25, 2011 Accepted: June 30, 2011

Introduction

Eukaryotes utilize changes in the cytosolic Ca^{2+} concentration ($[Ca^{2+}]_{cyt}$) as a second messenger to generate cellular responses to a wide variety of extracellular stimuli. In plants, Ca^{2+} has been implicated in transducing signals from various environmental changes into adaptive responses [1] by triggering rapid increases in $[Ca^{2+}]_{cyt}$ of a different magnitude and specialized character, which are not only transient but also vary spatially and temporally with different organelles or cytoplasmic regions acting as distinct compartments [2]. Thus, within cells a diverse array of changes in the $[Ca^{2+}]_{cyt}$ must be correctly perceived and discriminated so as to elicit the correct subsequent cellular response, a task performed in part by Ca^{2+}-modulated proteins.

For the majority of Ca^{2+}-modulated proteins, the Ca^{2+}-binding sites are composed of a characteristic helix–loop–helix motif called an EF-hand [3]. The EF-hand containing proteins are greatly diverse in terms of their structure, composition, Ca^{2+}-binding, and target interaction. In plants, genes encoding EF-hand containing proteins have been extensively annotated in *Arabidopsis thaliana* (L.) Heynh [4] and rice (*Oryza sativa* L.) [5]. An important group of proteins in the EF-hand family is the calmodulin (CaM) protein family, which transduces the signal of increased $[Ca^{2+}]_{cyt}$ by binding to and altering the activities of a variety of target proteins. This results in subsequent modulation of protein–protein interactions and the expression of target genes. CaM possesses two pairs of EF-hand domains connected by a long central helix giving it a dumbbell-shaped appearance [6]. The N- and C-terminal domains both contain a pair of EF-hand domains and bind Ca^{2+} cooperatively. Ca^{2+}-loaded CaM makes contact with its target proteins via large, surface-exposed hydrophobic patches in both globular domains of the molecule. Each hydrophobic patch is formed by many highly conserved methionine and phenylalanine residues, which are dispersed throughout the primary structure of CaM [7]. When the EF-hands of CaM bind Ca^{2+}, the exposed hydrophobic patches, in concert with the central helix, a flexible linker domain, facilitate the interaction of CaM with different target proteins.

A large family of *Cam* and *Cam-like* (*CML*) genes has been extensively identified from the two model plants, *A. thaliana* [8] and *O. sativa* [5]. Although the broad significance of these proteins can be postulated to be

important in distinguishing between the Ca^{2+} signals from different stimuli, and thus aid in eliciting the correct response, the actual significance is, however, not clearly understood. Until now, there is no detailed information on the biophysical and structural features of the *Cam* and *CML* gene products in rice, which is considered as a model plant for monocot and cereal plants. To understand the mechanisms by which Ca^{2+} signals, rich in both spatial and temporal information, are transduced, knowledge on the biophysical characteristics of their sensor proteins that help decode these complex signals is essential. Here, the recombinant proteins encoded by 11 such genes (3 *OsCam* and 8 *OsCML* genes) were produced in *Escherichia coli*, purified to apparent homogeneity, and assessed for their Ca^{2+} and target peptide binding ability, and their conformational changes on Ca^{2+}-binding through measurements by circular dichroism (CD) and fluorescence spectroscopy using 8-Anilino-1-naphthalene-sulfonic acid (ANS).

Materials and Methods

Sequence retrieval and analysis

Nucleotide and amino acid sequences were obtained from GenBank databases via the National Center for Biotechnology Information (http://www.ncbi.nlm.nih.gov/), and the rice databases including the MSU Rice Genome Annotation Project database [9] and the Rice Annotation Project Database [10]. Multiple sequence alignment was performed using ClustalW [11] via the European Bioinformatics Institute database (http://www.ebi.ac.uk).

Structure analysis

Comparative analysis was performed using structures from the Protein Data Bank (PDB; http://www.pdb.org/) as templates for homology prediction: Ca^{2+}-loaded N-CaM (2RO8), Ca^{2+}-loaded C-CaM (2RO9) [12], and Ca^{2+}-loaded N-Centrin (2AMI) [13]. The N- and C-terminal structures were predicted using the ExPaSy SWISS-MODEL program [14] and visualized by the 3D molecule viewer (Invitrogen, Carlsbad, USA). All predicted 3D structures were used for inter-helical angle calculation using the program INTERHLX [15].

Cloning of *OsCam* and *OsCML* genes

To clone *OsCam* and *OsCML* genes, polymerase chain reaction (PCR) was conducted using the cDNA clones obtained from the DNA Bank of NIAS (Japan) as the template. The forward and reverse primers for each gene, excluding *OsCam1,* including the 5′ flanking sequence with the restriction site for directional cloning of the PCR amplicon, were shown in **Table 1**, along with the GenBank accession number of the gene sequence used. For *OsCam1*, the previously reported expression clone (*OsCam1-1*) [16] was used. The mutant clone of *OsCML1* that lacked the sequence encoding the carboxyl-terminal extension, termed as *OsCML1d* was constructed by PCR using the indicated primers in **Table 1**.

PCR was performed in a total reaction volume of 50 μl and comprised of 0.2–0.5 mM dNTP, 0.2–0.5 μM of each primer, 2 mM Mg^{2+}, 0.1 μg of DNA, and 2 U of *Vent* DNA polymerase (NEB, Ipswich, USA) with an initial denaturation of 95°C for 10 min followed by 30 cycles of 95°C for 60 s, T_m–5°C for 45 s and 72°C for 90 s, and a final elongation at 72°C for 10 min. All PCR products were purified by agarose gel electrophoresis and cloned into pTZ57R (Promega, Fitchburg, USA) for amplification, and subsequently cloned into pET21a (Novagen, Darmstadt, Germany) for recombinant expression using appropriate restriction enzymes. Prior to expression, selected clones were confirmed for correct amplification

Table 1 Primers used for PCR-based amplification and cloning of the *OsCam* and *OsCML* genes

Gene	GenBank	Primer sequence (5′–3′)	
		Forward	Reverse
OsCam2	C73257	CCAACCC*CATATG*GCGGACC	CCCAAC*GGATCC*TATGCTCC
OsCam3	AU085804	G*CATATG*GCGGACCAGCTCA	AT*GGATCC*TGGAACTCCCCC
OsCML1	AU006154	CTGCT*CATATG*GCGGACCAG	GTGGA*GGATCC*TACTACACG
OsCML1d	AU006154	CTGCT*CATATG*GCGGACCAG	CTC*CTCGAG*CTTCACTTGGCCATC
OsCML3	AK111834	*CATATG*GACCACCTGACAAA	*GGATCC*TGAAACCTACATCT
OsCML4	AK067694	*CATATG*GAAGGGCTGACGAG	*GGATCC*ATGAACGGCATCTT
OsCML5	AU085804	CA*CATATG*GCGGAGGTGGAG	GAGA*GGATCC*TAATTATTGGTCGGA
OsCML8	AK065782	*CATATG*GCGAGCAAATACAGAGGC	*AAGCTT*AAAAAACCCGGCCCCA
OsCML9	AK105230	*CATATG*GCGGCCAAGCTGAC	*AAGCTT*CTTGTTGTTCATCAACACC
OsCML11	AK072726	*CATATG*AGCGAGCCGGCCCAC	*AAGCTT*GGAGAAGATGTTGTCAAATGC
OsCML13	AK074019	CTCC*CATATG*TCTACTGTCAAG	*AAGCTT*GTAACCATATCCAGTC

and absence of PCR/cloning mediated mutations by sequencing.

Recombinant protein production

Protein production in *E. coli* BL21 (DE3) was induced for 4 h by isopropyl β-D-thiogalactoside addition to a final concentration of 0.3 mM. The cells were harvested and resuspended in 50 mM Tris-HCl buffer (pH 7.5) containing 0.5 mM dithiothreitol and 1 mM ethylenediaminetetraacetic acid, sonicated and then centrifuged at 27 000 *g* for 50 min at 4°C. With the exception of OsCML9 for which Ni-column chromatography was used, protein purification was carried out using hydrophobic chromatography on phenyl-Sepharose (Amersham, Little Chalfont, UK). Binding and washing were carried out and proteins were eluted as reported [17]. The protein concentration was measured by the bicinchoninic acid assay (Pierce, Rockford, USA) using bovine serum albumin as standards. All proteins were dialyzed against sufficient ethylene glycol tetraacetic acid (EGTA) to remove Ca^{2+}.

Electrophoretic shift analyses

To perform the electrophoresis shift assay, 1 mM of $CaCl_2$ or 3 mM of EGTA was added to each protein (500 pmole) and mixed prior to resolution by 12% (w/v) sodium dodecyl sulfate–polyacrylamide gel electrophoresis (SDS–PAGE) and detected by Coomassie blue staining. To examine the peptide-binding ability, each protein (200 pmole) was mixed with the peptide (0–400 pmole) derived from CaM kinase II (CaMKII) (Sigma, St Louis, USA) in 100 mM Tris-HCl (pH 7.2) containing 1 mM $CaCl_2$ and 4 M urea, incubated for 1 h at room temperature, and then fractionated by 4 M urea denaturing 12% (w/v) SDS–PAGE and detected by Coomassie blue staining.

CD spectroscopy

CD spectroscopy was carried out at 25°C in a J-715 Spectropolarimeter (Jasco, Easton, USA) with constant N_2 flushing. The far-UV CD spectra were measured from 190 to 250 nm in 1 mM Tris-HCl (pH 7.5) and 1 mM KCl in the presence of 1 mM $CaCl_2$ or 1 mM EGTA. The final concentration of each protein used was 10 μM. All measurements were performed 30 min after sample preparation, using a 1-mm-path-length quartz cell with a 1 s response time, 50 mdeg sensitivity, 50 nm/min scan speed, and a 2.0 nm spectral bandwidth. The average of three scans was taken.

Fluorescence measurement

The fluorescence emission spectra of ANS (Sigma, St Louis, USA) were performed on an LS55 Luminescence Spectrometer (PerkinElmer, Waltham, USA) at 25°C. Fluorescence emission spectra were monitored with an excitation wavelength light of 370 nm and scan emission spectra in the range 400–650 nm. All measurements were performed using 1 μM of each protein in 1 mM Tris-HCl (pH 7.5) and 1 mM KCl with ANS at a final concentration of 100 μM in the presence of 1 mM $CaCl_2$ or 1 mM EGTA.

Results

Production of recombinant OsCaMs and OsCML proteins

To examine the biophysical properties of the three OsCaMs and eight closely related OsCMLs, the recombinant proteins were produced and purified to apparent homogeneity. Comparison of their deduced amino acid sequences by multiple sequence alignment is shown in **Fig. 1**. All these proteins contain four EF-hand domains, as one pair in each of the N- and C-terminal regions, with the exception of OsCML9 that contains only one EF-hand. While the three OsCaMs display very high amino acid sequence identity (97.3%–98.7%) with AtCaM3, the eight OsCMLs share 43.6%–84.6% identity with the typical plant CaM.

Based on this sequence alignment, three OsCMLs (OsCML8/11/13) contain an N-terminal extension harboring some unusual amino acid sequences. OsCML8 has a region of nine consecutive glycines followed by a region rich in arginine and lysine, OsCML11 has 10 consecutive glutamines, and OsCML13 has a region rich in positively-charged amino acids somewhat similar to OsCML8. On the other hand, two OsCMLs (OsCML1/3) contain a C-terminal extension consisting of a basic domain and a CAAX (C is cysteine, A is aliphatic, and X is a variety of amino acids) motif, a putative prenylation site [18]. In addition, an extra glycine-rich region (RGGENGGGGDDSGDAA) between the two pairs of EF-hand domains of OsCML5, and a region of eight consecutive glycines interrupting the supposed-to-be second EF-hand domain of OsCML9 are found. These unique sequence characteristics of these regions suggest that they may be structurally and functionally significant.

In this study, a truncated OsCML1 (OsCML1d) with its 38 amino acid extension removed was produced in order to determine its effect on the biophysical properties of OsCML1. With the exception of OsCML9, all recombinant proteins could be purified by Ca^{2+}-dependent hydrophobic chromatography as shown by the representative examples of OsCaM3 and OsCML13 in **Fig. 2(A,B)**, respectively. By SDS–PAGE, the apparent molecular weight (MW) of each recombinant protein produced agrees with the predicted MW from the deduced amino acid sequences.

Ca^{2+} and CaMKII peptide-binding properties

One of the characteristics of CaM is its ability to bind Ca^{2+} in the presence of SDS, which increases its

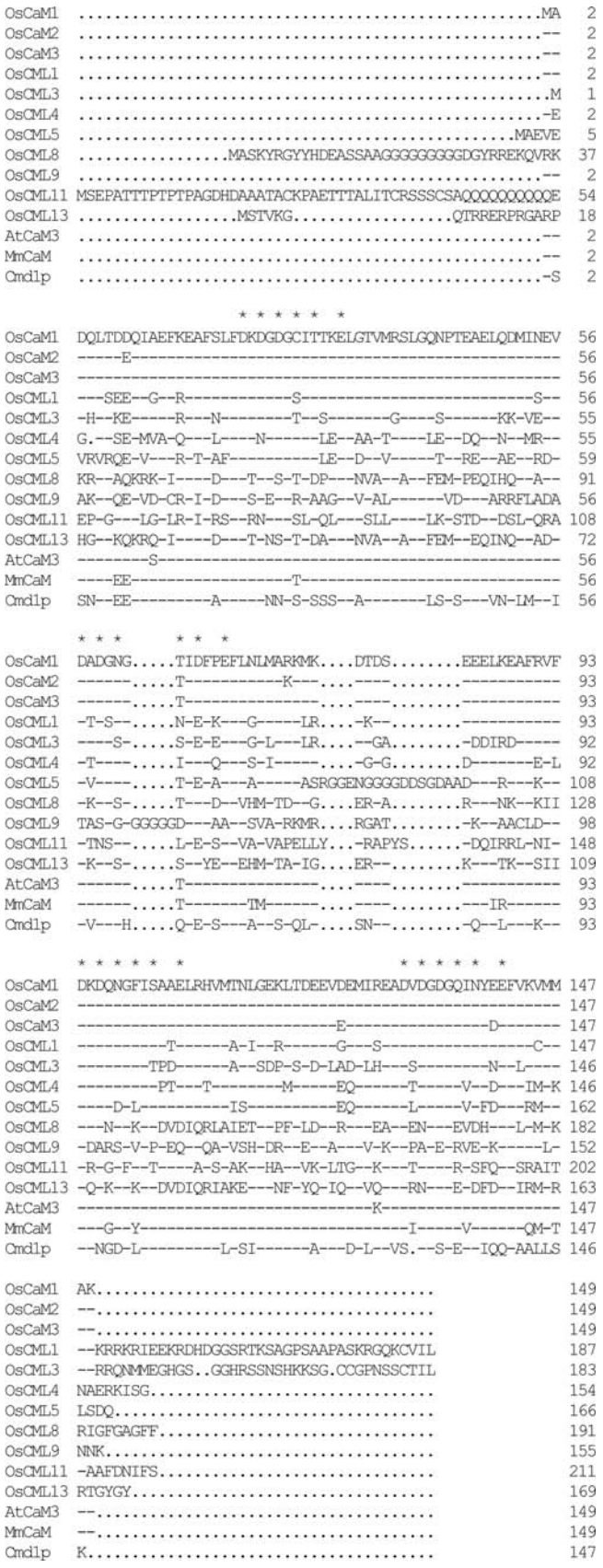

Figure 1 Comparison of the amino acid sequences of OsCaMs and OsCMLs The amino acid sequences of OsCaMs and OsCMLs were compared with those of *A. thaliana* (AtCaM3) (GenBank accession no. NP_191239), *Mus musculus* (MmCaM) (GenBank accession no. NP_033920), and *Saccharomyces cerevisiae* (CMD1p) (GenBank accession no. NP_009667) using OsCaM1 as a standard. Identical residues in other sequences are indicated by a dash (−), and a gap introduced for alignment purposes is indicated by a dot (.). Residues serving as Ca^{2+}-binding ligands (EF-hand domains) are marked with an asterisk (*).

electrophoretic mobility relative to CaM in the absence of Ca^{2+}. **Figure 2(C)** showed that all 11 recombinant proteins, plus the OsCML1d protein, displayed this shift when incubated with Ca^{2+}. The three OsCaMs, and four (OsCML4/5/8/13) of the eight OsCMLs exhibited a high degree of mobility shift, while OsCML9 and OsCML11 displayed only a subtle, but still discernable, change. The reduced mobility shift of OsCML9 matches its single EF-hand domain, as opposed to those proteins with four such domains, but any such correlation is offset by the observation that OsCML11 also has a weak mobility shift but four EF-hand domains. Even though the degree of mobility shift varies among the different recombinant proteins, these results indicate that OsCaMs and OsCMLs produced in *E. coli* and purified by Ca^{2+}-dependent hydrophobic chromatography are likely to be functional Ca^{2+}-binding proteins.

In addition, the ability to bind the peptide derived from CaM kinase II (CaMKII) was assessed by gel mobility shift assay. As CaMKII is a CaM-binding protein, examination of the ability of a CML to interact with its CaM-binding domain would suggest whether the CML potentially shares at least part of a similar set of binding proteins to CaM and may potentially be (but not have to be) redundant in terms of their functions. All three OsCaMs were found to display an altered electrophoretic mobility that could be distinguished from that of the free proteins, as shown by the representative results of OsCaM2 and OsCaM3 in **Fig. 2(D,E)**, respectively. The band shift indicates that they are likely to bind the CaMKII peptide and suggests that mechanisms of action of OsCaMs may well be, at least in part, similar to those from known typical CaMs. In contrast, under the same conditions, none of the eight OsCMLs displayed detectable band shifts upon incubation with the CaMKII peptide (data not shown), and so may not form complexes with the CaMKII peptide.

Analysis of structural changes from CD spectroscopy

Far-UV CD spectroscopy was used to determine the secondary structure of all recombinant proteins and whether any structural changes occurred upon Ca^{2+}

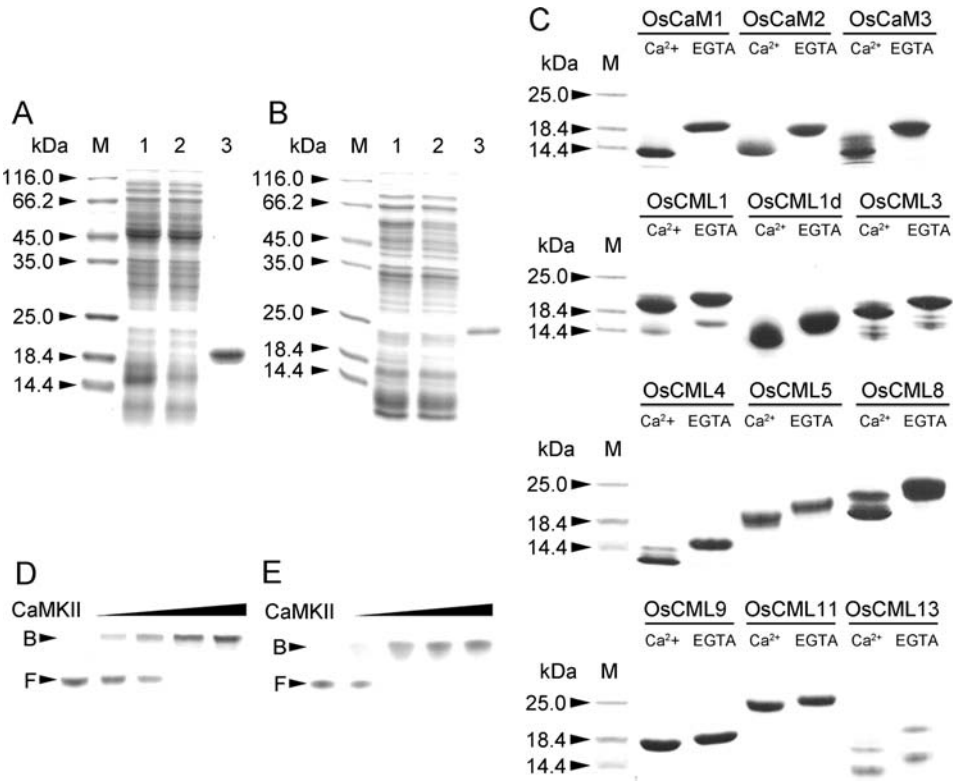

Figure 2 Analyses of the recombinant OsCaMs and OsCMLs (A,B) Separation by 12% (w/v) SDS-PAGE of proteins extracted from *E. coli* harboring pET21a expression plasmids following phenyl-sepharose hydrophobic chromatography of OsCaM3 (A) and OsCML13 (B). Lane M, molecular mass standard proteins (Fermentas, Waltham, USA); lane 1, crude extract; lane 2, flow-through fraction; lane 3, eluted protein. (C) Calcium-induced electrophoretic mobility shift analysis of all recombinant proteins examined. Each protein in the presence of 1 mM $CaCl_2$ ($+Ca^{2+}$) or 3 mM EGTA (+EGTA) was subject to SDS-PAGE. Lane M, molecular mass standard proteins (Fermentas). (D,E) Gel mobility shift analysis of OsCaM2 (D) and OsCaM3 (E) after incubation with increasing amounts (indicated by closed triangle) of CaMKII peptide and then resolved by denaturing 4 M urea/SDS-PAGE. Gels shown are representative of three repeated experiments.

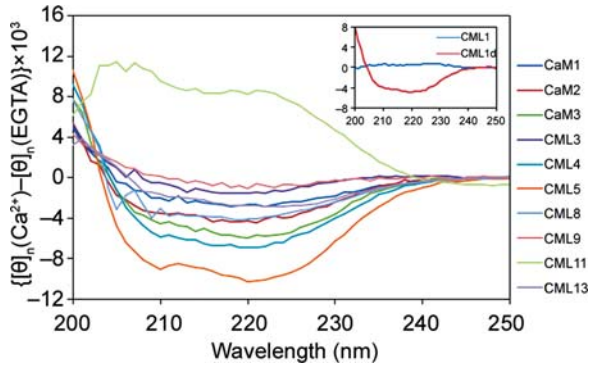

Figure 3 Ca^{2+}-induced conformational changes of OsCaMs and OsCMLs measured by far-UV CD spectroscopy The spectra were recorded in 1 mM Tris-HCl (pH 7.5) in the presence of 1 mM $CaCl_2$ or 1 mM EGTA and presented as the calculated CD difference spectrum, $[\theta]_n$ in the presence of Ca^{2+} minus $[\theta]_n$ in the presence of EGTA for each protein (10 μM). Insets were the CD difference spectra of OsCML1 and OsCML1d. Spectra shown are representative of three independent experiments.

binding. For CaM, the major reported conformational changes include an increase in the α-helicity upon Ca^{2+} binding [19,20], whereas very little structural information is available for the CMLs. The far-UV CD spectra of all proteins in the presence of Ca^{2+} or EGTA have two minima near 208 and 222 nm (**Supplementary Figure S1**), indicating that these proteins contain substantial α-helical structure. For each protein, the CD difference spectrum calculated from the mean residue ellipticity ($[\theta]_n$) in the presence of Ca^{2+} minus that in the presence of EGTA, is shown in **Fig. 3**. On Ca^{2+} addition, a change in the $[\theta]_n$ at 208 and 222 nm was clearly observed for all three OsCaMs and for five (OsCML4/5/8/11/13) of the eight OsCMLs, with OsCML1, OsCML3, and OsCML9 displaying very little change. However, the truncated form of OsCML1 (OsCML1d) showed a clear increment in the $[\theta]_n$ in the presence of Ca^{2+}, which is in contrast to the full sized OsCML1 protein.

Table 2 summarizes the values of θ_{222} from the spectra of all proteins in the presence or absence of Ca^{2+} and thus their changes on Ca^{2+} addition. All OsCaMs displayed a large increase in the molar ellipticity of >20% in the presence of Ca^{2+} when compared with those in the absence of Ca^{2+}, indicating that the helical content was highly increased in these proteins upon Ca^{2+} binding. In contrast, OsCML1, which shares a high amino acid sequence identity (84.6%) with typical CaMs, did not exhibit this induction,

Table 2 Far-UV CD and ANS fluorescence measurements of OsCaMs and OsCMLs

Protein	Far-UV CD			ANS fluorescence		
	$[\theta_n]_{222}\times10^3$ (deg·cm^2/dmole·number of residues)[a]		$[\theta_n]_{222}$ (+Ca^{2+})/$[\theta_n]_{222}$ (+EGTA)[b]	Emission maximum (nm)	$\triangle\lambda^c_{max}$	I_{max} (+Ca^{2+})/I_{max} (+EGTA)[d]
	+Ca^{2+}	+EGTA				
OsCaM1	−14.35	−11.50	1.24	464	45	3.02
OsCaM2	−17.48	−13.37	1.30	469	44	4.28
OsCaM3	−16.99	−11.17	1.52	466	48	4.26
OsCML1	−9.50	−10.09	0.94	475	37	5.02
OsCML1d	−12.55	−7.79	1.61	470	44	4.67
OsCML3	−16.31	−14.76	1.11	468	46	4.75
OsCML4	−17.82	−11.03	1.62	480	34	1.81
OsCML5	−17.62	−7.53	2.34	484	33	2.28
OsCML8	−21.33	−17.42	1.22	480	8	1.59
OsCML9	−17.17	−16.43	1.04	502	8	1.08
OsCML11	−14.30	−22.81	0.63	476	30	2.08
OsCML13	−19.92	−17.08	1.16	477	38	2.57

[a]The mean residue ellipticity at 222 nm; [b]The ratio of the mean residue ellipticity at 222 nm in the presence of Ca^{2+} to that in the presence of EGTA; [c]The difference of maximum emission of ANS between in the presence of Ca^{2+} and in the presence of EGTA; [d]The ratio of the maximum fluorescence intensity of ANS in the presence of Ca^{2+} to that in the presence of EGTA.

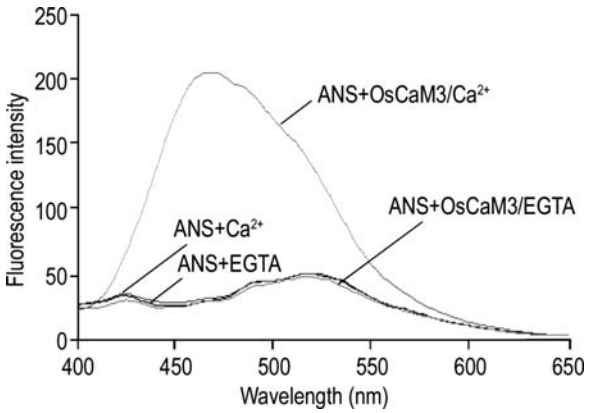

Figure 4 Conformational changes of the representative example of OsCaM3 measured by ANS fluorescence Emission spectra of 100 μM ANS in the absence and in the presence of 1 μM of OsCaM3 protein were monitored at an excitation wavelength of 370 nm. The spectra were recorded in 1 mM Tris-HCl (pH 7.5) in the presence of 1 mM $CaCl_2$ or 1 mM EGTA. Spectra shown are representative of three independent experiments.

while OsCML3, whose sequence is 64.9% identical to that of typical CaMs, exhibited only a small increase (11%). Interestingly, when the C-terminal extension of OsCML1 was truncated (i.e. OsCML1d), a large increase (61%) in molar ellipticity was observed. In contrast with the other proteins, the CD spectrum in the presence of Ca^{2+} of OsCML11 displayed a significant decrease (>37%) in the molar ellipticity at 208 and 222 nm, yet, similar to the other proteins, its peak height at the interval of 190–200 nm substantially increased in the presence of Ca^{2+}.

Measurement of ANS fluorescence

ANS is a fluorescent probe that displays a blue shift when its environment is changed from an aqueous to a non-polar media. In addition, while its fluorescence in water is usually weak, ANS shows an enhanced intensity when it is in a non-polar media. Therefore, ANS is a useful probe for the Ca^{2+}-induced exposure of the hydrophobic patches in the globular domains of CaMs. To examine this exposure, the emission spectra of ANS in the presence of each protein with or without Ca^{2+}, were monitored with an excitation wavelength of 370 nm. When mixed with each protein in the presence of EGTA, ANS displayed a relatively weak fluorescence with a maximum wavelength near 520 nm, which is almost identical to that of ANS alone either with or without Ca^{2+} with the exception of OsCML8 and OsCML9. For these proteins, a significant difference between the ANS alone and ANS mixed with the protein was observed suggesting their ability to interact with target proteins at resting levels of Ca^{2+}. **Figure 4** shows a representative result of the emission spectra of ANS in an aqueous buffer mixed with OsCaM3 protein. With the exception of OsCML9, when Ca^{2+} was added, the aforementioned fluorescence changes were clearly observed indicating the exposure of hydrophobic patches of all OsCaMs and OsCMLs. **Table 2** summarizes ANS fluorescence in the presence of each recombinant protein. In the presence of Ca^{2+}, the fluorescence spectrum of ANS mixed with each of the three OsCaMs and the two most highly conserved OsCMLs (OsCML1/3), exhibited significant blue shifts in the maximum emission wavelengths

Table 3 Interhelical angles in OsCaMs and OsCMLs

Protein	I/II	I/III	I/IV	II/III	II/IV	III/IV
Ca^{2+}-CaM1-N	105.5	−139.4	117.3	114.1	−33.9	101.0
Ca^{2+}-CaM1-C	99.4	−135.1	112.3	124.4	−47.4	105.4
Ca^{2+}-CaM2-N	105.4	−139.5	117.2	114.1	−34.0	100.9
Ca^{2+}-CaM2-C	99.4	−135.1	112.3	124.4	−47.4	105.4
Ca^{2+}-CaM3-N	105.5	−139.4	117.3	114.1	−33.9	101.0
Ca^{2+}-CaM3-C	99.4	−135.1	112.2	124.4	−47.3	105.5
Ca^{2+}-CML1-N	105.4	−139.6	117.1	114.1	−34.0	100.9
Ca^{2+}-CML1-C	99.5	−135.0	112.2	124.4	−47.4	105.5
Ca^{2+}-CML3-N	105.4	−139.5	117.1	114.2	−34.1	101.0
Ca^{2+}-CML3-C	100.0	−134.9	112.2	124.0	−46.9	105.7
Ca^{2+}-CML4-N	105.8	−139.3	117.2	113.9	−33.5	101.1
Ca^{2+}-CML4-C	99.4	−135.1	111.2	124.4	−51.5	104.7
Ca^{2+}-CML5-N	105.7	−139.5	117.2	113.8	−34.2	100.9
Ca^{2+}-CML5-C	99.3	−135.1	112.1	124.5	−47.4	105.5
Ca^{2+}-CML8-N	120.0	−120.8	124.2	113.7	−29.9	114.7
Ca^{2+}-CML13-N	119.9	−120.8	124.1	113.8	−30.1	114.8

(from 37 to 46 nm) and relatively large concomitant increases in the intensity (3.0−5.0-fold). OsCML1d also exhibited broadly similar changes to the full-length OsCML1. With the exception of OsCML9, on Ca^{2+} addition, the rest of the OsCMLs also caused similar changes to the ANS fluorescence, however, with smaller blue shifts and lower levels of intensity increment. Nonetheless, the changes indicate that these OsCMLs expose hydrophobic patches on their surfaces on Ca^{2+} binding.

Structural comparison of OsCaM and OsCML proteins

Comparative analysis was carried out using structures from the PDB as templates for homology prediction of the N- and C-terminal domains of the OsCaM and OsCML proteins. Interhelical angles among the four α-helices within each domain were calculated using the program INTERHLX [15]. The results shown in **Table 3** indicate that all structures possess an open conformation with all OsCaMs and the highly conserved OsCMLs (OsCML1/3/4/5) having similar respective interhelical angles, which suggests their structural similarities. The more diverged OsCML8 and OsCML13 also occupy the open conformation but with a lesser degree of Ca^{2+}-induced opening of the EF-hand domains. An interesting question is whether OsCaMs and the highly conserved OsCMLs are redundant or they possess unique functionality. If the latter was the case, how could one explain the functional diversity of these proteins? CaM functions by exposing its hydrophobic surfaces that interact with its target proteins upon Ca^{2+} binding, so another important feature of CaM to be considered is the amino acid distribution on these target-binding surfaces. Therefore, the hydrophobic target-binding sites of these proteins were compared as shown in **Fig. 5**. All proteins examined have extensive hydrophobic surfaces containing clusters of several methionine residues. In contrast to OsCaMs whose overall structures appear identical to one another, OsCMLs have different patterns of amino acid distribution within their putative target-binding sites. The N-terminal domains display more diverse patterns of methionine distribution than the C-terminal domains with the exception of OsCML4 and OsCML5, in which a larger cluster of methionine residues, compared with OsCaMs, occupies the hydrophobic surface of their C-terminal domain. In addition, the positively and negatively charged residues surrounding the putative target-binding sites, which also contribute to the target binding, are uniquely distinct among the more diverged OsCML proteins.

Discussion

Even though the biophysical and biochemical properties of CaMs have been known in some plant species, those of their related calcium sensors, CMLs, have not been explored. This work reported the biophysical properties of the 3 CaM proteins and 8 CML proteins encoded by 11 genes from the rice genome. All recombinant proteins displayed the characteristic gel mobility shift in the presence of Ca^{2+}, *albeit to* a varying degree. Based on the results of protein purification by Ca^{2+}-dependent hydrophobic chromatography and Ca^{2+}-induced gel mobility shift, as well as the structural changes deduced from CD spectroscopy and ANS fluorescence, these proteins, with the exception of OsCML9, appear to bind Ca^{2+} and undergo certain structural changes on doing so.

Arbitrarily, five genes which encode three different proteins that share the highest degree of amino acid sequence identity with known typical plant CaMs have been classified as *OsCam,* while 32 CaM-related calcium sensors have been annotated as *OsCML* [5]. To examine the possible differential target-binding characteristics, which are indicative of how they can be classified, their ability to bind the peptide derived from CaM kinase II in the presence of Ca^{2+} was assessed. All three OsCaMs exhibited this ability, while all eight OsCMLs examined did not bind the peptide even though some of them share as high as 85% amino acid sequence identity with the OsCaMs. These results suggest to some extent that the target proteins of OsCMLs are likely to be at least in part different from, though maybe overlapping, with those of OsCaMs and support the annotation of the proteins encoded by five highly conserved *OsCam* genes as 'true' CaM.

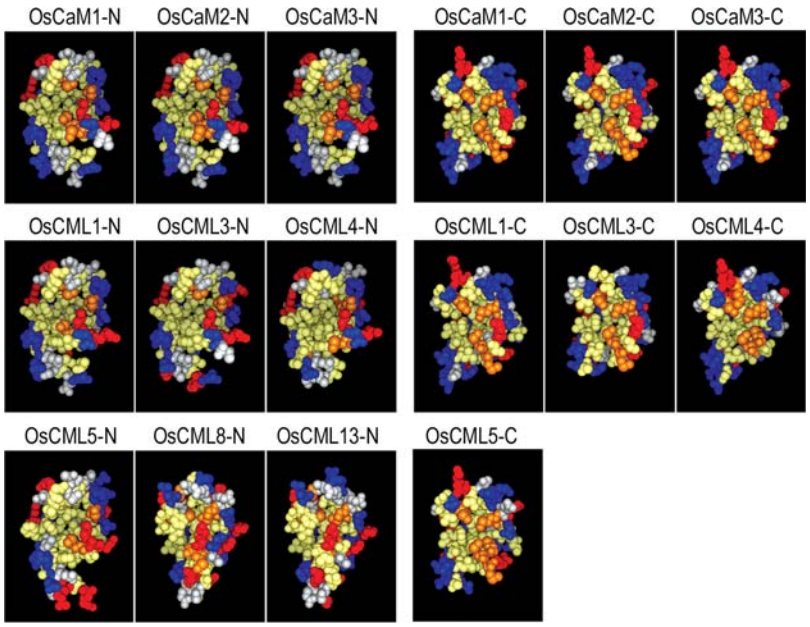

Figure 5 Comparison of the putative target-binding surfaces between the Ca^{2+}-bound OsCaMs and Ca^{2+}-bound OsCMLs Space-filling representation displays target-binding sites occupied by the hydrophobic (yellow) and methionine (orange) residues. The surrounding positive and negative residues are highlighted in blue and red, respectively.

Among the eight OsCMLs examined, excluding their C-terminal extension, OsCML1 and OsCML3 share the highest-sequence identities with OsCaM1 and contain a high percentage of conserved methionines (4.3% and 4.9%). These characters reflect in the obtained ANS fluorescence in which their emission maximum is significantly shifted and the intensity increased in the presence of Ca^{2+}. However, the CD spectra of OsCML1 and OsCML3 did not reveal an obvious increase in the helical content on Ca^{2+}-binding, suggesting that their mechanism of Ca^{2+}-induced structural change is potentially different from that of the OsCaMs. When OsCML1 was truncated, it displayed a large increase in the molar ellipticity upon Ca^{2+} binding, suggesting that the 38-amino-acid C-terminal extension plays an important role in regulating the conformational change. OsCML1, also known as OsCaM61, was reported to be membrane-associated when it is prenylated and localized in the nucleus when it is unprenylated [21]. We speculate that its association with the membrane by its C-terminal extension causes Ca^{2+}-induced conformational changes that are different from those of the free protein and may subsequently confer the membrane-associated OsCML1 the ability to interact with different target proteins.

OsCML4 and OsCML5, which share very-high-sequence identities with OsCaM1 (68.9% and 66.2%), and contain a high methionine percentage (6.5% and 4.8%), were found to behave very similarly to the OsCaMs except that, on Ca^{2+}-binding, their ANS emission maxima did not increase as much. Among the proteins examined, OsCML5 displayed the highest degree of change in its molar ellipticity (134%) in the presence of Ca^{2+}, even more so than the three OsCaMs. OsCML5 has some interesting features, namely the extra region rich in glycine between its two EF-hand pairs. This structure likely affects the conformational change of OsCML5 as well as how it interacts with target proteins, because this structure interrupts the central helix, of which its flexibility is key to the mechanism of the protein action.

OsCML8 and OsCML13, which share lower sequence identities with OsCaM1 (47.0% and 43.6%), exhibited only a small increase in their molar ellipticity of the CD spectrum as well as a smaller blue shift and intensity increment of the ANS fluorescence emission maxima. Small changes in the ANS fluorescence in the presence of these proteins were observed despite the fact that they possess a very high percentage of methionines (5.2% and 5.3%, respectively), most of them in the same positions as in OsCaM1. OsCML8 and OsCML13 are two out of only three OsCMLs in which one of their EF-hands contains aspartate at residue 12. The presence of aspartate in this position instead of glutamate is believed to raise the affinity for Mg^{2+} by 10-fold [22] and likely affects the Ca^{2+}-binding kinetics of OsCML8 and OsCML13. In addition, both proteins also contain extra positively charged amino acid sequences on the N-terminal end, of which their regulatory functions are speculated.

OsCML11, which shares only 44.1% sequence identity with OsCaM1, displayed similar Ca^{2+}-dependent changes in the ANS fluorescence as that seen in OsCML4 and OsCML5, but in contrast displayed a decreased molar ellipticity in the presence of Ca^{2+} indicating that OsCML11 was more helical in the Ca^{2+}-free conformation than in the

Ca^{2+}-bound state. In contrast to the other proteins that contain four EF-hands, OsCML11 did not clearly exhibit the Ca^{2+}-induced gel mobility shift. Interestingly, OsCML11 contains a low percentage of methionines (1.4%) and when its amino acid sequence was closely inspected, aliphatic amino acids (leucine, valine, and isoleucine) were found instead at the corresponding methionine positions in typical CaMs. Methionine has a greater conformational flexibility compared with leucine, valine, and isoleucine and is weakly polarized, allowing interaction with highly polarized solvents, such as water, and target proteins in a sequence-independent manner [7]. The presence of aliphatic amino acids would likely cause the exposed surface to be less flexible and so only be able to interact with more specific target proteins. OsCML11 shares a high amino acid sequence identity with AtCML18, which was found localized in the plant vacuolar compartment with a function of modifying the activity of a Na^+/H^+ exchanger (AtNHX1) in a Ca^{2+}- and pH-dependent manner [23].

From the structural comparison, OsCML proteins examined have nearly identical overall main-chain conformation to OsCaMs, but contain some distinct charged and hydrophobic amino acid distribution on their target-binding site. These features are likely responsible for the multifunctionality of the OsCaM and OsCML protein family. Similarly, Ikura and Ames [24] have examined structure and target recognition of NCS and S100 proteins, which revealed that their main-chain globular folds are nearly identical, but an important distinguishing structural property is the distribution of charged and hydrophobic side-chains on the protein surface. This genetic polymorphism has likely promoted the functional diversity among the OsCaM and OsCML family members.

CML proteins are a novel family of Ca^{2+}-binding proteins that possibly play critical roles in Ca^{2+}-mediated stress responses in plants. Like other plants, *O. sativa* possesses a large family of genes encoding CaMs and their related calcium sensor CMLs. For nearly all of these proteins, their structures and functions have not been previously explored. This report showed that all three OsCaMs exhibited typical characteristics of CaM, confirming their likely functionality as typical CaMs. Conversely, the OsCMLs exhibited a spectrum of both structural and functional characteristics that ranged from typical to atypical of CaMs. These results suggest that OsCMLs represent sensor proteins whose modes of actions are probably different from, although maybe overlapping with, those of OsCaMs and possibly serve distinct roles.

Supplementary Data

Supplementary data are available at *ABBS* online.

Acknowledgements

We thank Dr. Robert Butcher, PCU, Faculty of Science, Chulalongkorn University, for useful comments, and English proofreading and editing.

Funding

This work was supported by a grant from the Thailand Research Fund (RSA5280015) to T.B. and by the Graduate School, Chulalongkorn University through the 90th Year Anniversary of Chulalongkorn University Fund (Ratchadaphiseksomphot Endowment Fund) to S.T. This work was additionally supported by the Higher Education Research Promotion and National Research University Project of Thailand, Office of the Higher Education Commission (FW656B), and the A1B1 project of the Faculty of Science, Chulalongkorn University.

References

1 White PJ and Broadley MR. Calcium in plants. Ann Bot 2003, 92: 478–511.
2 McAinsh MR and Pittman JK. Shaping the calcium signature. New Phytol 2009, 181: 275–294.
3 Kretsinger RH and Nockolds CE. Carp muscle calcium-binding protein. J Biol Chem 1973, 248: 3313–3326.
4 Day IS, Reddy VS, Shad Ali G and Reddy ASN. Analysis of EF-hand-containing proteins in *Arabidopsis*. Genome Biol 2002, 3: research0056.1–0056.24.
5 Boonburapong B and Buaboocha T. Genome-wide identification and analyses of the rice calmodulin and related potential calcium sensor proteins. BMC Plant Biol 2007, 7: 4.
6 Chattopadhyaya R, Meador WE, Means AR and Quiocho FA. Calmodulin structure refined at 1.7 Å resolution. J Mol Biol 1992, 228: 1177–1192.
7 O'Neil KT and DeGrado WF. How calmodulin binds its targets: sequence independent recognition of amphiphilic α-helices? Trends Biochem Sci 1990, 15: 59–64.
8 McCormack E and Braam J. Calmodulins and related potential calcium sensors of Arabidopsis. New Phytol 2003, 159: 585–598.
9 Ouyang S, Zhu W, Hamilton J, Lin H, Campbell M, Childs K and Thibaud-Nissen F, *et al*. The TIGR rice genome annotation resource: improvements and new features. Nucleic Acids Res 2007, 35(database issue): D883–D887.
10 Tanaka T, Antonio BA, Kikuchi S, Matsumoto T, Nagamura Y, Numa H and Sakai H, *et al*. The Rice Annotation Project Database (RAP-DB): 2008 update. Nucleic Acids Res 2008, 36(database issue): D1028–D1033.
11 Thompson JD, Gibson TJ, Plewniak F, Jeanmougin F and Higgins DG. The CLUSTAL_X windows interface: flexible strategies for multiple sequence alignment aided by quality analysis tools. Nucleic Acids Res 1997, 25: 4876–4882.
12 Ishida H, Huang H, Yamniuk AP, Takaya Y and Vogel HJ. The solution structures of two soybean calmodulin isoforms provide a structural basis for their selective target activation properties. J Biol Chem 2008, 283: 14619–14628.
13 Sheehan JH, Bunick CG, Hu H, Fagan PA, Meyn SM and Chazin WJ. Structure of the N-terminal calcium sensor domain of centrin reveals the biochemical basis for domain-specific function. J Biol Chem 2006, 281: 2876–2881.

14 Kiefer F, Arnold K, Künzli M, Bordoli L and Schwede T. The SWISS-MODEL repository and associated resources. Nucleic Acids Res 2009, 37(database issue): D387–D392.
15 Yap KL, Ames JB, Swindells MB and Ikura M. Vector geometry mapping: a method to characterize the conformation of helix-loop-helix calcium binding proteins. Methods Mol Biol 2002, 173: 317–324.
16 Phean-o-pas S, Limpaseni T and Buaboocha T. Structure and expression analysis of the *OsCam1-1* calmodulin gene from *Oryza sativa* L. BMB Rep 2008, 41: 771–777.
17 Liao B and Zielinski RE. Production of recombinant plant calmodulin and its use to detect calmodulin binding proteins. Methods Cell Biol 1995, 49: 487–500.
18 Maurer-Stroh S and Eisenhaber F. Refinement and prediction of protein prenylation motifs. Genome Biol 2005, 6: R55.
19 Martin SR and Bayley PM. The effects of Ca^{2+} and Cd^{2+} on the secondary and tertiary structure of bovine testis calmodulin. A circular-dichroism study. Biochem J 1986, 238: 485–490.
20 Maune JF, Beckingham K, Martin SR and Bayley PM. Circular dichroism studies on calcium binding to two series of Ca^{2+} binding site mutants of *Drosophila melanogaster* calmodulin. Biochemistry 1992, 31: 7779–7786.
21 Dong A, Xin H, Yu Y, Sun C, Cao K and Shen WH. The subcellular localization of an unusual rice calmodulin isoform, OsCaM61, depends on its prenylation status. Plant Mol Biol 2002, 48: 203–210.
22 Cates MS, Teodoro ML and Phillips GJ, Jr. Molecular mechanisms of calcium and magnesium binding to parvalbumin. Biophys J 2002, 82: 1133–1146.
23 Yamaguchi T, Aharon GS, Sottosanto JB and Blumwald E. Vacuolar Na^+/H^+ antiporter cation selectivity is regulated by calmodulin from within the vacuole in a Ca^{2+}- and pH-dependent manner. Proc Natl Acad Sci USA 2005, 102: 16107–16112.
24 Ikura M and Ames JB. Genetic polymorphism and protein conformational plasticity in the calmodulin superfamily: two ways to promote multifunctionality. Proc Natl Acad Sci USA 2006, 103: 1159–1164.